Journal of Polymer Research (2020) 27: 56
https://doi.org/10.1007/s10965-020-2030-z

ORIGINAL PAPER

Bio-based cross-linked polyitaconamides synthesized through a Michael ene-amine addition and bulk polycondensation

Kuan Liang[1] · Jingbo Zhao[1] · Ganggang Zhang[1] · Zhiyuan Zhang[1] · Ling Shi[1] · Junying Zhang[1]

Received: 21 September 2019 / Accepted: 31 January 2020 / Published online: 10 February 2020

Abstract

A simple method is established to synthesize bio-based cross-linked polyitaconamides (cPITAs) through a Michael ene-amine addition and bulk polycondensation. A tetraester, i.e. tetramethyl piperazine-N,N′-bis(2-methylene butanedioate) (TMPB), was synthesized through a Michael addition of dimethyl itaconate and piperazine at 90 °C. Bulk polycondensation of TMPB with butanediamine or hexamethylenediamine was conducted at 130–170 °C under atmospheric pressure, and several cPITAs with tunable properties were prepared. The Michael addition and the polycondensation were monitored by FT-IR and ^{1}H NMR spectra. The cPITA films were characterized by DSC, WAXS, TGA, dynamic mechanical analysis, and tensile test. cPITAs exhibited T_g ranging from 58 to 72 °C, tensile strength up to 85 MPa, and strain at break from 9% to 17%.

Keywords Bio-based · Polyitaconamides · Michael ene-amine addition · Bulk polycondensation · Cross-linked polyamides

Introduction

Polyamides (PAs) exhibit high thermal stability, chemical resistance and mechanical durability. They play a vitally important role in engineering thermoplastics [1, 2]. PAs have been commercialized over 70 years. Typical PAs such as nylon-6, nylon-66, nylon-610 and nylon-12 are widely used as fibers and engineering plastics in various industrial sectors. Meanwhile, thermoplastic polyamide elastomers may also be prepared when polyether soft segments are introduced [3, 4].

With the diversification of demands, crosslinked polyamides (cPAs) are also developed gradually. cPAs have three-dimensional cross-linked structure. They show dimensional stability, high intermolecular force, good mechanical property, and insolubility in organic solvents. cPAs are used mainly as oil-resistant coatings, hot melt adhesives [5], composites [6, 7], and separating membranes [8]. cPAs are synthesized commonly through three methods: melt ring-opening polymerization-crosslinking method [9], melt polycondensation-crosslinking method [6], and solution polycondensation from diamine (DA) and polyacid halides [10]. cPAs recently attract increasing attentions in PA field. Researches on new synthesis methods, properties, and applications of cPAs increase evidently in this decade [11–16]. Liu et al. synthesized thermally reversible cPA gels from maleimide-containing PAs and a trifunctional furan compound [17]. Tylkowski et al. synthesized microcapsules constructed with liquid crystalline cPA shells, which exhibited nematic phase at 166 °C and excellent thermostability up to 340 °C [18]. The microcapsules showed photo-triggered release character. Trigo-López et al. introduced reactive azide groups into aromatic PA fibers, and improved the thermal and mechanical properties by simple thermal treatment [11]. Yi et al. synthesized cPAs through a Michael ene-amine addition and bulk polycondensation from methyl acrylate and diamines [19]. The cPAs exhibited good tensile strength up to 71 MPa.

Scientists also explore many methods synthesizing bio-polyamides. Different bio-based PAs have been synthesized as environmentally friendly alternatives to petroleum-based materials [20–23]. Itaconic acid is a bio-resource monomer. It can be synthesized via carbohydrate fermentation with Aspergillus terreus [24, 25]. Itaconic acid and its esters are

✉ Jingbo Zhao
zhaojb@mail.buct.edu.cn

✉ Junying Zhang
zhangjy@mail.buct.edu.cn

[1] Key Laboratory of Carbon Fiber and Functional Polymers (Beijing University of Chemical Technology), Ministry of Education, College of Materials Science and Engineering, Beijing University of Chemical Technology, Beijing 100029, China

usually used as vinyl monomers in radical polymerization to synthesize vinyl polymers [26–28]. Polycondensation between itaconic acid and diamines was also investigated to synthesize linear polyitaconamides [29–31]. However, up to now, cross-linked polyitaconamides (cPITAs) have not yet been reported.

In this paper, cPITAs with tunable properties were synthesized through a Michael ene-amine addition and bulk polycondensation. A tetraester, i.e. tetramethyl piperazine-N,N′-bis(2-methylene butanedioate) (TMPB), was synthesized through the Michael addition of dimethyl itaconate (DMI) with piperazine (PZ). Bulk polycondensation of TMPB with butanediamine (BDA) or hexamethylenediamine (HDA) was followed, and several cPITAs were prepared. The influence of structure, reaction temperature, and reaction time on the properties of cPITAs was investigated. DMI is the methyl ester of biobased itaconic acid. BDA, HDA, and PZ are normally prepared from petroleum resources. Recent studies show that they can also be prepared through bio-based ways. BDA is called putrescine, a bio-diamine. It has been prepared from glucose fermentation with engineered *Escherichia coli* [32]. HDA is usually prepared from the hydrogenation of adipamide, an amination derivative of adipic acid (AA) that can be prepared by metabolizing lignin with P. *putida* KT2440-JD1 [33]. PZ is an amination derivative of 2-chloro-ethanol, which is prepared usually from the addition reaction of ethylene with HClO, while ethylene can be prepared from the dehydration of bio-ethanol. Hence cPITAs may be prepared from bio-based starting materials. Meanwhile, different from the literature [19] in which a mixture containing four hexanediamine multi-esters was used as crosslinker, a pure diaminetetraester, i.e. TMPB, was synthesized and used to prepare cPITAs.

Experimental

Materials

DMI (97 wt%) and PZ (99 wt%) were commercially obtained from Alfa Aesar Chemical Co. Ltd. BDA (99 wt%) was purchased from Acros Chemical Co., Ltd., Belgium. HDA (99 wt%) was purchased from Aladdin Chemical Co. Ltd., China.

Synthesis of TMPB

In a 100 mL three-necked flask, 1.72 g (0.02 mol) PZ and 6.33 g (0.04 mol) DMI were added at a PZ/DMI molar ratio of 1:2 and were stirred at 90 °C for 3 h under nitrogen atmosphere. After cooled at room temperature, pale yellow TMPB solid (crude yield: 96%) was obtained. The crude product was recrystallized with ethyl alcohol-petroleum ether mixture solvent (1:1 *v*/v). The yield of pure TMPB was 67%. Its melting point is 103 °C.

Synthesis of cPITAs

cPITAs were designated as DA-T_p-T_c-*t*, in which DA represents HDA or BDA, T_p represents the polycondensation temperature in fluid state, T_c represents the curing temperature in film state, and *t* represents the curing or crosslinking time. cPITAs were prepared under similar conditions (Table 1) with the TMPB/(HDA or BDA) molar ratio of 1:2. For example, HDA-170-170-15 was synthesized as follows:

In a 100 mL three-necked flask, 4.02 g (0.01 mol) TMPB and 2.35 g (0.02 mol) HDA were heated at 170 °C under reflux state in nitrogen atmosphere for 1 h. A viscous PITA preolymer was obtained, and then was poured into tetrafluoroethylene molds of different shapes. The samples were transferred into a vacuum oven (170 °C). A reduced pressure of 30 mmHg was applied for 30 min to eliminate the bubbles in the liquid films. Crosslinking was conducted for 15 h under atmospheric pressure at 170 °C. A series of 50 × 4 × 1 mm rectangle or 60× 4 × 1 mm dumbbell HDA-170-170-15 films were prepared.

Characterization

FT-IR spectra were conducted on a NICOLET 60SXB FTIR spectrometer with KBr compression pellets. ^{1}H NMR spectra were acquired on a Bruker 400 AVANCE with samples dissolved in *d*6-DMSO by using tetramethylsilane as the internal standard. ESI-MS spectra were recorded on Agilent Technologies 6540 UHD Accurate-Mass Q-TOF LC/MS spectroscope with samples dissolved in methanol. A Rigaku D/Max 2500 VB2+/PC diffractometer was adopted to get wide angle X-ray scattering (WAXS) curves with Cu $K\alpha$ radiation. TA Q200 differential scanning calorimeter was used to get differential scanning calorimetry (DSC) curves in a cooling (10 °C/min)-heating (10 °C/min) process under N_2. Thermogravimetric analysis (TGA) was performed on a TGA Q50 analyzer at a heating rate of 10 °C/min in N_2 atmosphere. 60 × 4 × 1 mm dumbbell-shaped samples were used in the mechanical analyses conducted on a Lloyd LR30K tensile testing machine at a 5 mm/min tensile speed. 50 × 4 × 1 mm rectangle samples were used for dynamic mechanical analyses (DMA) performed on a TA Q800 machine at a heating rate of 3 °C/min under N_2. The amplitude and frequency were 5 μm and 1 Hz, respectively. About 0.50 g of samples were refluxed in 10 mL of DMF for 2.5 h. The undissolved solid was filtered, washed with ethanol, dried, and weighed. Then, gel percentage was calculated (Table 1).

Table 1 Preparation of cPITAs

cPITAs (DA-T_p-T_c-ts)	DA	Bulk polycondensation [a] temperature, T_p (°C)	Curing reaction		Gel percentage (%)
			Temperature, T_c (°C)	Time, t (h)	
HDA-170-170-15	HDA	170	170	15	85.1
HDA-170-160-15	HDA	170	160	15	66.4
HDA-170-130-40	HDA	170	130	40	76.6
BDA-130-130-40	BDA	130	130	40	61.3
BDA-150-130-40	BDA	150	130	40	70.6
BDA-170-130-40	BDA	170	130	40	79.0
BDA-170-130-25	BDA	170	130	25	48.2
BDA-170-130-15	BDA	170	130	15	32.1
BDA-170-120-40	BDA	170	120	40	51.6

[a] Bulk polycondensation time in fluid state under reflux: 1 h

Results and discussion

Synthesis of TMPB

As we all know, monomer functionality is of great importance for the preparation of cross-linked polymers. In order to prepare cPITAs, a new bio-based crosslinker, TMPB, was prepared by a Michael ene-amine addition of DMI and PZ at 90 °C according to a similar reference [34]. The preparation process is shown as Scheme 1.

The Michael addition between DMI and PZ is confirmed by monitoring the variation of absorption peaks corresponding to the C=C in DMI and the N − H in PZ. Before addition reaction (0 h), the absorptions at 1637 cm^{-1} (νC=C) and 1555 cm^{-1} (δN-H) are easily observed (Fig. 1). As the reaction proceeded, both of them became weak. When the addition was conducted for 3 h, the C=C and N − H peaks became nearly negligible. Result reveals that Michael addition is easily conducted at 90 °C.

In the ^{1}H NMR monitoring spectra of Michael addition (Fig. 2), the peaks at 5.85 and 6.20 ppm correspond to the C=CH_2 hydrogens in DMI, while the peaks at 2.96 and 2.31 ppm correspond to the -CH_2-N and –OOC-CH– hydrogens in TMPB; respectively. With the reaction proceeding, the C=CH_2 peak decreases, whereas the -CH_2-N and –OOC-CH- peaks increase. Michael addition between C=C and –NH bonds is very swift. When DMI and PZ were mixed at 90 °C (0 h), this addition occurred immediately, with some TMPB formed. After 3 h, Michael addition was nearly completed.

The molecular weight of addition product at 3 h was detected by ESI-MS spectrum (Fig. 3). A strong peak was found at the m/z of 403. It is related to the M + 1 of TMPB, of which M is 402 g/mol. TMPB is nearly a pure compound with melting point at 103 °C (Fig. 4).

Synthesis of cPITAs

TMPB and HDA or BDA were first reacted in flasks to get viscous prepolyamides. Then, they were poured into tetrafluoroethylene molds for further crosslinking. cPITA films with different shapes were prepared (Scheme 2).

The T_p was 170 °C for the HDA-derived cPITAs, while the T_p was 130, 150, and 170 °C, respectively, for the BDA-derived cPITAs. Bulk polycondensation was conducted in the flask under reflux state. Although T_p was up to 170 °C which was above the boiling point (b.p.) of BDA (160 °C), the evaporated BDA could also be condensed into the flask and the bulk polycondensation was not influenced. The time of bulk polycondensation was mainly determined based on the viscosity of prepolymers. For the BDA series with higher reactivity, when bulk polycondensation time was above 1 h,

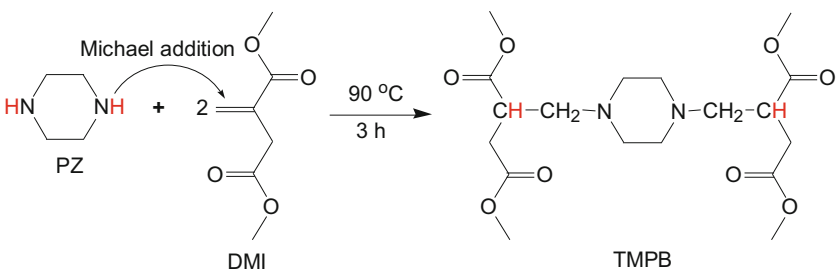

Scheme 1 Synthesis of TMPB through a Michael addition of PZ and DMI at a molar ratio of 1:2

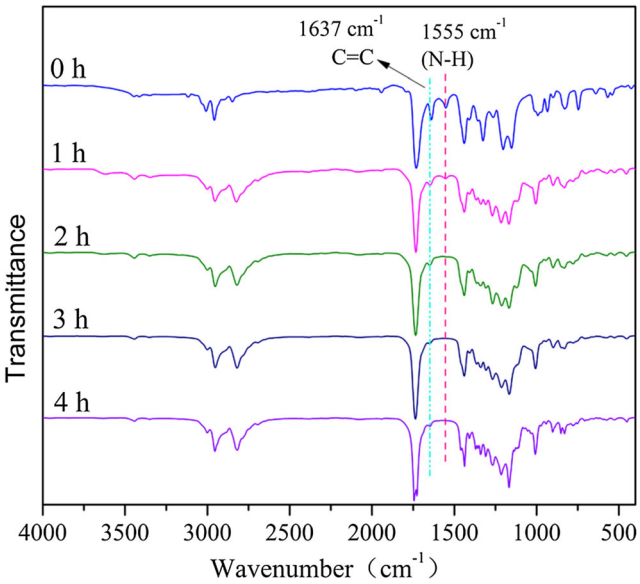

Fig. 1 FT-IR monitoring spectra of the Michael addition (PZ/DMI molar ratio, 1:2; 90 °C; bulk)

the viscosity of prepolymers was too high to flow. Thus, the bulk polycondensation was stopped at 1 h. The T_c in curing stage was selected at 130, 160, and 170 °C for HDA-derived cPITAs. High T_c profits high curing rate (Table 1). Restricted by low b.p. of BDA, BDA-derived cPITAs was crosslinked at lower T_c of 120–130 °C to avoid the volatilization of residue BDA. However, lower T_c made BDA-derived cPITAs crosslinked slowly. Thus, longer curing time was needed.

The curing time (t) was determined by FT-IR tracking. In FT-IR spectra, when the strength of ester peak (decrease) and amide peak (increase) became unchanged, we believed that the curing reaction was completed. The FT-IR monitoring spectra of HDA-170-170-15 (Fig. 5(a)) revealed that ester

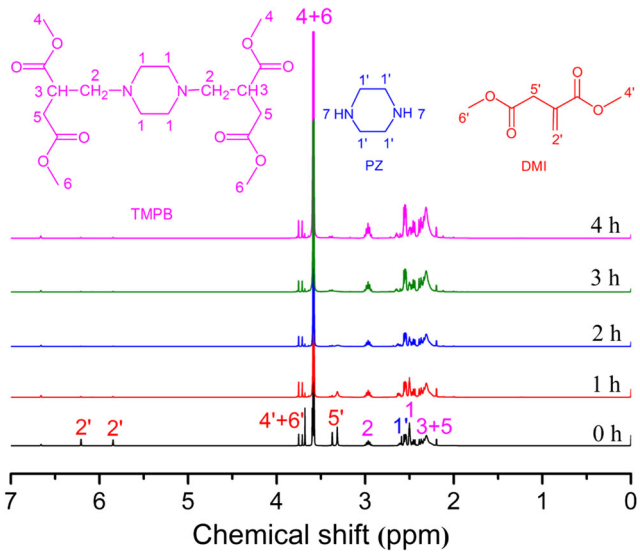

Fig. 2 ^{1}H NMR (*d*6-DMSO) monitoring spectra of the Michael addition between PZ and DMI (PZ/DMI molar ratio, 1:2; 90 °C; bulk)

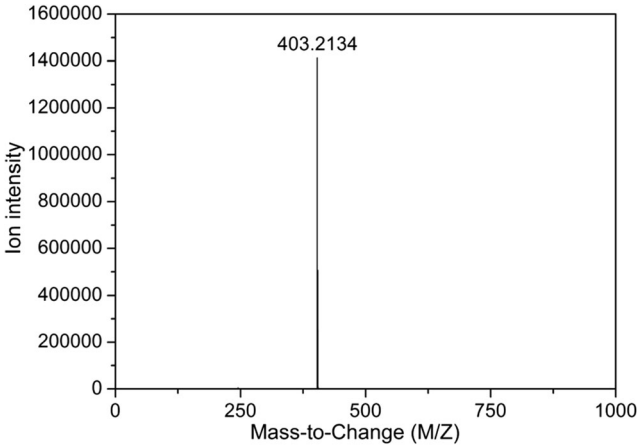

Fig. 3 ESI-MS spectrum of the components in Michael addition after 3 h (PZ/DMI molar ratio, 1:2; 90 °C; bulk)

νC=O peak (1736 cm^{-1}) was still strong at 1 h in polycondensation stage, while a strong amide νC=O peak appeared (1699 cm^{-1}). After 8 h in film curing stage, the ester νC=O peak disappeared. Longer curing time leaded to the increase of amide νC=O peak. At the same polycondensation time (1 h) and temperature (170 °C) in fluid state, the ester νC=O peak in BDA-170-130-40 became very weak, with a strong amide νC=O peak appeared (1663 cm^{-1}) (Fig. 5 (b)). Polycondensation between TMPB and BDA is much faster than that between TMPB and HDA, maybe because short BDA exhibits lower steric hindrance and higher polarity which make BDA react easier with TMPB during refluxing polycondensation stage. When prepolyamides were transferred into vacuum oven and crosslinked in film state, curing between TMPB and HDA was still fast due to higher T_c (170 °C). 15 h curing time was sufficient to get highly crosslinked HDA-170-170-15. BDA-170-130-40 was cured

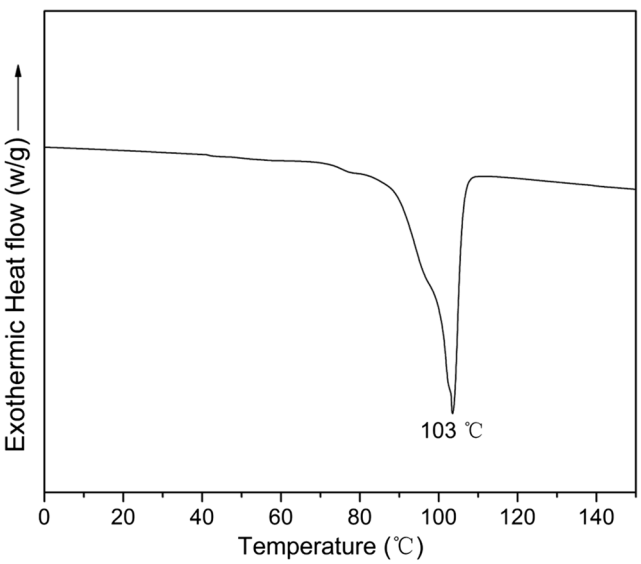

Fig. 4 Heating DSC scan of pure TMPB

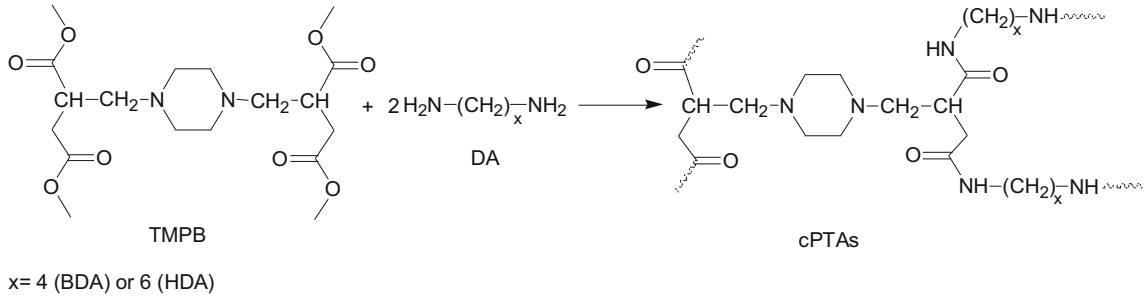

Scheme 2 cPITAs synthesized through bulk polycondensation of TMPB with HDA or BDA

at 130 °C. Lower T_c caused longer curing time and lower crosslinking extent (Table 1).

After bulk polycondensation was conducted in flask under reflux (170 °C, 1 h), BDA-170-130-40 was characterized by ^{1}H NMR spectrum (Fig. 6). The spectrum revealed that polycondensation between BDA and TMPB took place. At this point, BDA-170-130-40 consisted mainly of polyitaconamide structures (II), with a little portion of structure (I) or ester groups left. Peaks at 7.78 and 8.05 ppm correspond to the –CONH- protons in polyitaconamide structures (II), while peak at 3.59 ppm correspond to the –$COOCH_3$ in structure (I). In Fig. 6, peak 11 is obviously stronger than peak 13 (peak 11/peak 13 area ratio: 1.67). It means that methyl 4 in structure (I) is more reactive than methyl 6. As the ester group connected on –CH = is closer to PZ unit than the ester group on –CH_2-, the former ester is more affected by the electron-withdrawing effect of PZ unit. Thus, methyl 4 shows higher reactivity than methyl 6.

It is well known that linear or hyperbranched polymers are soluble in some solvents, and cross-linked polymers are insoluble in any solvents. Using this property, the gel percentage of cPITAs was detected by refluxing them in DMF for 2.5 h [19]. Results are listed in Table 1. HDA-170-170-15 was prepared at the T_p and T_c all of 170 °C. It shows the highest gel percentage of 85.1%. It crosslinked more completely than others. HDA-170-160-15 was prepared at the same T_p (170 °C) but lower T_c of 160 °C. Its gel percentage or crosslinking extent is lower than that of HDA-170-170-15. HDA-170-130-40 was prepared at lower T_c of 130 °C and longer t of 40 h. Long t also

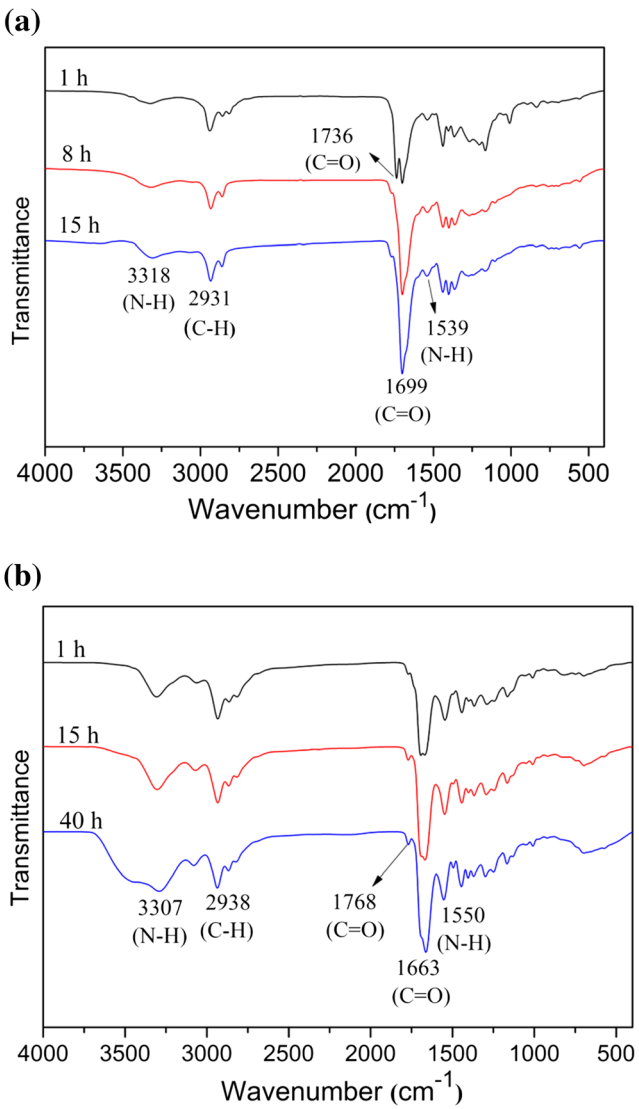

Fig. 5 FT-IR monitoring spectra of HDA-170-170-15 (a) and BDA-170-130-40 (b) in the polycondensation and curing stage

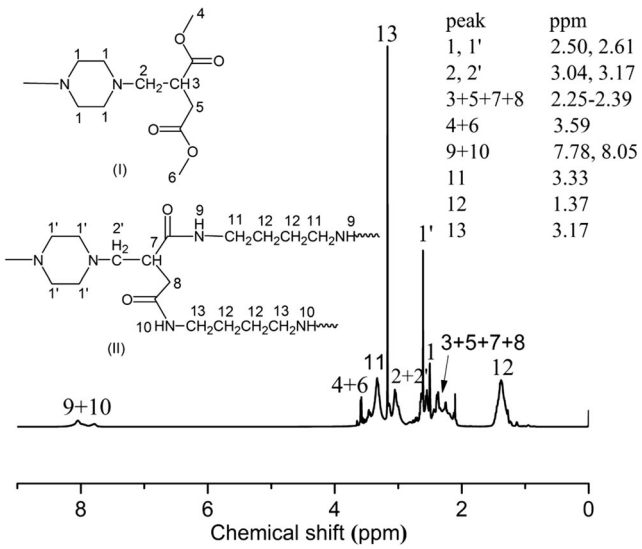

Fig. 6 ^{1}H NMR (*d*6-DMSO, room temperature) spectrum of BDA-170-130-40 after 1 h in the polycondensation stage

resulted in high gel percentage. BDA-130-130-40 was prepared at T_p and T_c all of 130 °C. Its gel percentage is relatively low at 61.3% because low T_p and T_c caused low crosslinking extent. At the same T_c (130 °C), higher T_p also benefits the crosslinking. BDA-170-130-40, BDA-170-130-25 and BDA-170-130-15 were prepared at the same T_p and T_c. Longer t also led to higher gel percentage. Meanwhile, BDA-170-120-40 showed obvious lower gel percentage than BDA-170-130-40. Their T_p was the same (170 °C), but the T_c of BDA-170-120-40 was lower. Low T_c causes lower crosslinking extent or gel percentage.

DSC and WAXS characterization

In the DSC scans of cPITAs (Fig. 7), no crystallization peaks were observed. BDA-derived cPITAs show higher glass transition temperature (T_g) than HDA-derived cPITAs (Table 2) because shorter BDA forms more rigid BDA-diamide units. From the analysis of the first three samples based on BDA-derived cPITAs, it is found that T_p does not affect T_g. The reason is that T_g is affected by the final crosslinking state of cPITAs. When TMPB and HDA or BDA were refluxed in flask at different T_ps after 1 h polycondensation, viscous prepolyamides were obtained. Although the viscosity of prepolyamides was different, they were still fluids. Thus, the T_p did not affect the T_g of final cPITAs. Figure 8 also reveals that T_c and t influence T_g. Lower T_c and shorter t all caused lower crosslinking extent and lower T_g.

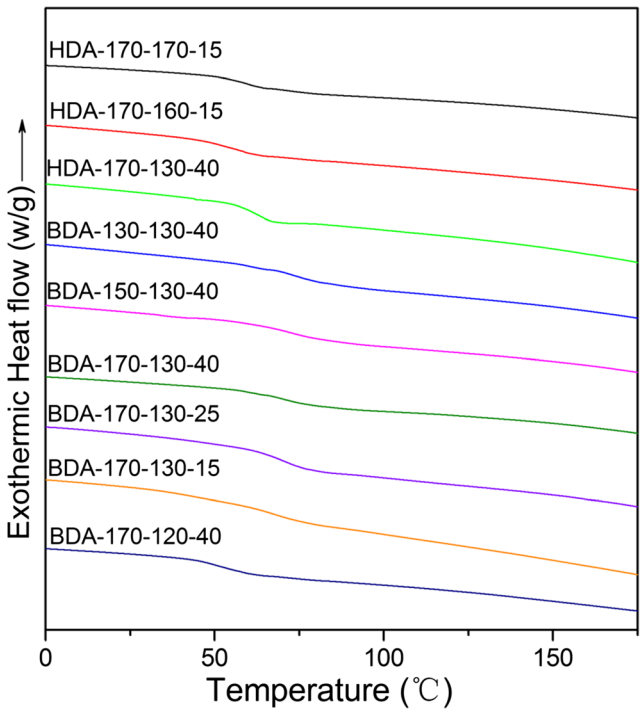

Fig. 7 DSC heating scans of cPITAs detected in a cooling (10 °C/min)-heating (10 °C/min) process

Figure 8 shows the WAXS curves of cPITAs. cPITAs except HDA-170-170-15 and BDA-170-130-40 all exhibit a tiny crystallization peak at the 2θ of about 22.0 °, which corresponds to the crystallization of linear polyamides [35]. These cPITAs were synthesized at lower T_p, T_c or t, which caused incomplete crosslinking. Linear polyamide segments formed during polycondensation and curing period were not completely crosslinked. Some of them still remained in free state and had the ability to crystallization. Thus, a crystallization peak emerged. HDA-170-170-15 and BDA-170-130-40 were synthesized at higher T_p, T_c or t. Their crosslinking extent was high. Crosslinking connected the linear polyamide segments all together and made their crystallization difficult. Thus, amorphous HDA-170-170-15 and BDA-170-130-40 were obtained.

DMA characterization

cPITAs show one or two $T_{\alpha 1}$s in the 10–75 °C range and one or two $T_{\alpha 2}$s in the 75–150 °C range (Fig. 9, Table 2), whereas $T_{\alpha 1}$s and $T_{\alpha 2}$s correspond to the low cross-linking units and high cross-linking units [36]; respectively. cPITAs are in the glassy state below $T_{\alpha 1}$ with E' above 1000 MPa. As temperature rises, low cross-linking units move first, and some motion energy is needed, leading to $T_{\alpha 1}$s appeared and E' decreased. Subsequently, with further increase of temperature, high cross-linking units begin to move, leading to $T_{\alpha 2}$s appeared and E' decreased further. HDA-170-170-15 shows one $T_{\alpha 1}$ and one $T_{\alpha 2}$ [Fig. 9(a), Table 2] maybe because HDA-170-170-15 forms similar amount of low cross-linking units and high cross-linking units. HDA-170-160-15 shows two $T_{\alpha 1}$s without $T_{\alpha 2}$ because low T_c merely leaded to low crosslinking units. HDA-170-130-40 shows two $T_{\alpha 2}$s without $T_{\alpha 1}$. Although its T_c was lower, longer t also leaded to high cross-linking units. BDA-130-130-40, BDA-150-130-40 and BDA-170-130-40 were synthesized at the same T_c (130 °C). As T_p increased, their $T_{\alpha 1}$ and the lower $T_{\alpha 2}$ increased more or less [Fig. 9(b), Table 2]. Higher T_p benefits the polycondensation and the followed crosslinking, with low and high cross-linking units all increased. BDA-170-130-25 and BDA-170-130-15 were synthesized at the same T_p and T_c as BDA-170-130-40. Short t caused the decrease of the lower $T_{\alpha 2}$ or the appearance of $T_{\alpha 1}$ (for BDA-170-130-15). This meant the decrease of high cross-linking units or the appearance of low cross-linking units. BDA-170-120-40 and BDA-170-130-40 was prepared at the same T_p. Lower T_c caused BDA-170-120-40 showing a strong $T_{\alpha 1}$ and a weak $T_{\alpha 2}$, maybe because higher amount of low cross-linking units and lower amount of high cross-linking units were formed in BDA-170-120-40. Low T_c or short t leads to low crosslinking extent.

Table 2 DSC and DMA data of cPITA films

cPITAs	T_g (DSC) (°C)	T_α (DMA)	
		$T_{\alpha1}$ (in 10–75 °C range)	$T_{\alpha2}$ (in 75–150 °C range)
HDA-170-170-15	60	64	112
HDA-170-160-15	58	36,62	–
HDA-170-130-40	61	–	77, 94
BDA-130-130-40	72	50	81,106
BDA-150-130-40	72	58	89,107
BDA-170-130-40	72	51	93
BDA-170-130-25	71	–	89,101
BDA-170-130-15	68	63	90,101
BDA-170-120-40	61	27	93

TGA characterization

Sharp weight losses in TGA curves (Fig. 10(a)) are closely consistent with two degradation stages or two decomposition peaks (T_{d1} and T_{d2}) in the DTGA curves (Fig. 10(b)). HDA-derived cPITAs show higher T_{d1}, T_{d2}, and weight loss temperature at 5% (T_5%) than BDA-derived cPITAs (Table 3). Thermal stability is mainly determined by the amount of less thermally stable amide linkages in cPITAs, whether or not these amide linkages are in linear or crosslinked structural units. HDA has longer –CH_2- chain than BDA. This makes HDA-derived cPITAs contains lower amide amount than BDA-derived cPITAs in per unit weight. Thus, HDA-derived cPITAs show higher thermal stability than BDA-derived cPITAs. Some cPITAs show a tiny peak between 80 and 210 °C because of incomplete crosslinking. Further polycondensation between remaining -NH_2 and -$COOCH_3$ groups still proceeds in this period, with a little portion of CH_3OH released. Particularly, BDA-170-120-40 loses more weight in this stage due to the lowest T_c. Decomposition between 200 and 400 °C is related to the scission of amide linkages (T_{d1}),

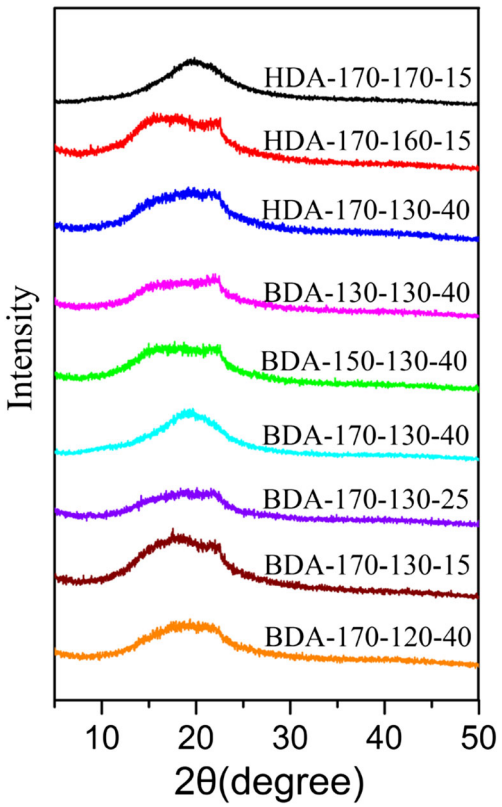

Fig. 8 WAXS curves of cPITAs

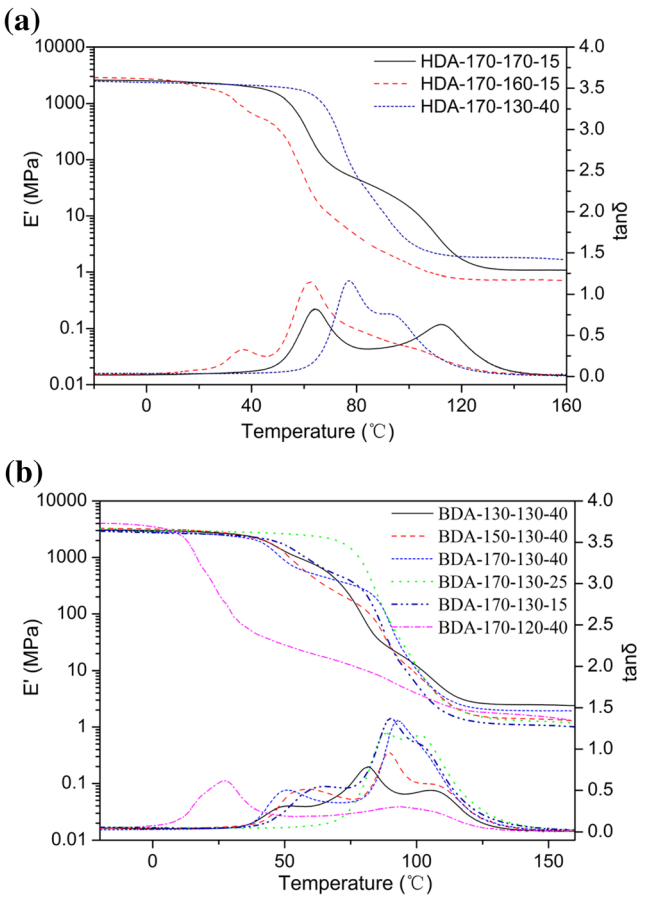

Fig. 9 *E′* and tan*δ* curves of HDA-derived cPITAs (**a**) and BDA-derived cPITAs (**b**)

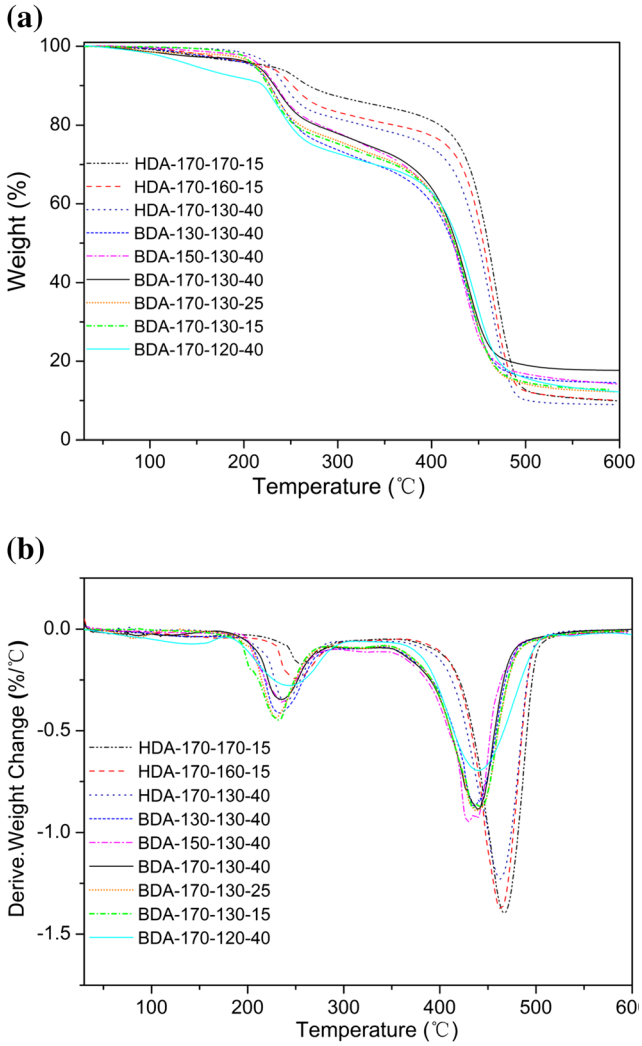

Fig. 10 TGA (**a**) and DTGA (**b**) curves of cPITAs

while the decomposition between 400 and 500 °C corresponds to the scission of C-C linkages (T_{d2}). HDA-derived cPITAs commonly show weaker T_{d1} and stronger T_{d2} also because of their higher thermal stability. cPITAs are thermally stable cross-linked polyamides below 210 °C except BDA-170-120-40.

Tensile testing

cPITAs exhibits strong stress of 29.9–84.6 MPa (Table 3). T_g has great influence on the mechanical properties of cPITAs. Amide linkages in linear and crosslinked units all act on the stiffness and intermolecular interactions of cPITAs. As HDA has longer $-CH_2-$ chain than BDA, HDA-derived cPITAs contains lower amide amount than BDA-derived cPITAs in per unit weight. This makes HDA-derived cPITAs show lower T_g and weaker intermolecular interactions. Thus, HDA-derived cPITAs show lower tensile strength than BDA-150-130-40 and BDA-170-130-40 (Fig. 11). Meanwhile, crosslinking extent or gel percentage also influences mechanical properties. BDA-170-120-40 shows higher tensile strength than BDA-170-130-15 because the former has higher gel percentage. T_p and T_c all influence gel percentage, and also influence the mechanical properties. At the same curing time, high T_c resulted in high gel percentage (Table 1) and tensile strength. Similar results are observed between HDA-170-170-15 and HDA-170-160-15 or BDA-170-130-40 and BDA-170-120-40. T_p also has certain effect on the mechanical properties. In BDA-derived cPITAs, the higher the T_p is, the higher the tensile strengths are. High T_p causes fast reaction rate and high final crosslinking degree. BDA-170-130-40, BDA-170-130-25 and BDA-170-130-15 were synthesized at the same T_p and T_c. High curing time leads to high T_g and high tensile strength due to high crosslinking extent.

Conclusion

A series of bio-based crosslinked polyitaconamides, cPITAs, with outstanding mechanical properties were successfully synthesized from a tetraester, tetramethyl piperazine-N,N′-bis(2-methylene butanedioate), with hexamethylenediamine and butanediamine. cPITAs exhibit T_g from 58 to 72 °C. Short chain length of diamines and high curing temperature or longer curing time all cause high T_g. T_g has great influence

Table 3 TGA (Heating rate, 10 °C/min under N_2) and tensile testing data of cPITAs

Samples	$T_{5\%}$ (°C)	T_{d1} (°C)	T_{d2} (°C)	End mass (%)	Tensile strength (MPa)	Strain at break (%)
HDA-170-170-15	227	255	467	9.9	60.6	12.5
HDA-170-160-15	225	251	463	10.0	37.3	11.5
HDA-170-130-40	228	242	462	9.7	62.4	14.0
BDA-130-130-40	212	231	435,443	14.5	59.4	14.2
BDA-150-130-40	214	236	428,440	14.1	68.9	17.4
BDA-170-130-40	212	233	440	17.7	84.6	17.4
BDA-170-130-25	214	229	439	12.3	48.3	10.5
BDA-170-130-15	211	232	435,443	12.7	29.9	9.1
BDA-170-120-40	146	240	439	12.1	42.9	14.7

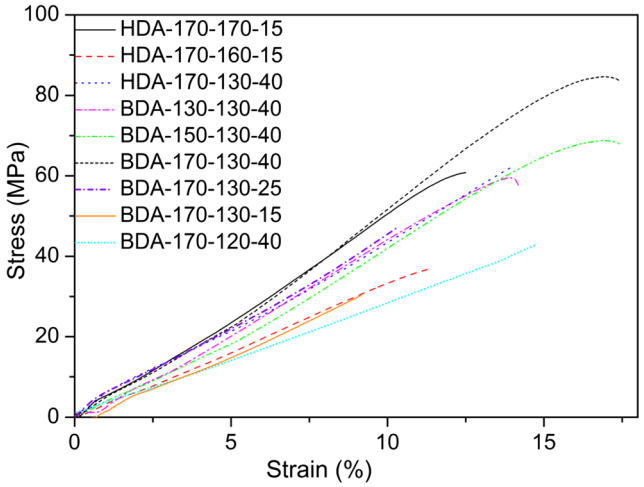

Fig. 11 Stress-strain curves of cPITAs

on the mechanical properties of cPITAs. High T_g usually leads to high tensile strength. High polycondensation temperature in liquid stage also improves the mechanical properties of cPITAs. cPITAs with excellent tensile strength up to 84.6 MPa were synthesized through bulk Michael ene-amine addition and polycondensation from dimethyl itaconate, piperazine, and hexamethylenediamine or butanediamine. These cPITAs may be used as coatings, composites, and separating membranes.

Acknowledgments This work was financially supported by Beijing Natural Science Foundation (No. 2182056) and National Natural Science Foundation of China (Grant No. 21244006).

References

1. Pervaiz M, Faruq M, Jawaid M, Sain M (2017) Polyamides: developments and applications towards next-generation engineered plastics. Curr Org Synth 14:146–155
2. García JM, García FC, Serna F, de la Peña JL (2010) High-performance aromatic polyamides. Prog Polym Sci 35:623–686
3. Sole BB, Lohkna S, Chhabra PK, Prakash V, Seshadri G, Tyagi AK (2018) Preparation of mechanically strong poly (ether block amide)/mercaptoethanol breathable membranes for biomedical applications. J Polym Res 25:200/1–200/12
4. Kong WB, Yang YY, Liu ZM, Lei JX (2017) Structure-property relations of novel polyamide-6 elastomers prepared through reactive processing. J Polym Res 24:168/1–168/9
5. Gordon RL (2001) Warming up to polyamides. Adhesives Age 44(12):39–40 42-43
6. Howland CP, Bailey KM, Workman DP, Moeggenborg KJ (1999) Crosslinked polyamide binders for ceramics, ceramic precursor, and its manufacture. PCT Int Appl WO 9928377:A1
7. Bradler PR, Fischer J, Wallner GM, Lang RW (2018) Characterization of irradiation crosslinked polyamides for solar thermal applications-basic thermo-analytical and mechanical properties. Polymers (Basel, Switzerland) 10(9):969/1–969/11
8. Zhang Y, Liu YQ, Pan GY, Yan H, Xu J, Guo M (2017) Antisoiling composite reverse osmosis membranes and preparation method and applications thereof. Faming Zhuanli Shenqing CN 107297158 A
9. Philippe D, Bernd B, Dietrich S, Andreas W, Andreas R (2013) Process for producing polyamides via anionic polymerization. US patent 2013079465A1
10. Williams JC, Meador MAB, McCorkle L, Mueller C, Wilmoth N (2014) Synthesis and properties of step-growth polyamide aerogels cross-linked with triacid chlorides. Chem Mater 26:4163–4171
11. Trigo-López M, Barrio-Manso JL, Serna F, García FC, García JM (2013) Crosslinked aromatic polyamides: a further step in high-performance materials. Macromol Chem Phys 214:2223–2231
12. Li M, Bijleveld J, Dingemans TJ (2018) Synthesis and properties of semi-crystalline poly(decamethylene terephthalamide) thermosets from reactive side-group copolyamides. Eur Polym J 98:273–284
13. Feulner R, Brocka Z, Seefried A, Kobes MO, Hulder G, Osswald TA (2010) The effects of e-beam irradiation induced cross linking on the friction and wear of polyamide 66 in sliding contact. Wear 268:905–910
14. Kong LY, Shan WD, Han SL, Zhang T, He LC, Huang K, Dai S (2018) Interfacial engineering of supported liquid membranes by vapor cross-linking for enhanced separation of carbon dioxide. Chem Sus Chem 11:185–192
15. Leisen C, Drummer D (2016) Infrared welding of cross-linkable polyamide 66. Express Polym Lett 10:849–859
16. Zhao YL, Zhang ZG, Dai L, Mao HC, Zhang SB (2017) Enhanced both water flux and salt rejection of reverse osmosis membrane through combining isophthaloyl dichloride with biphenyl tetraacyl chloride as organic phase monomer for seawater desalination. J Membr Sci 522:175–182
17. Liu YL, Hsieh CY, Chen YW (2006) Thermally reversible cross-linked polyamides and thermo-responsive gels by means of Diels–Alder reaction. Polymer 47:2581–2586
18. Tylkowski B, Pregowska M, Jamowska E, Garcia-Valls R, Giamberini M (2009) Preparation of a new lightly cross-linked liquid crystalline polyamide by interfacial polymerization. Application to the obtainment of microcapsules with photo-triggered release. Eur Polym J 45:1420–1432
19. Yi CF, Zhao JB, Zhang ZY, Zhang JY (2017) Cross-linked polyamides synthesized through a Michael addition reaction coupled with bulk polycondensation. Ind Eng Chem Res 56:13743–13750
20. Pagacz J, Raftopoulos KN, Leszczyńska A, Pielichowski K (2015) Bio-polyamides based on renewable raw materials. J Therm Anal Calorim 123:1225–1237
21. Song L, Zhu T, Yuan L, Zhou J, Zhang Y, Wang Z, Tang C (2019) Ultra-strong long-chain polyamide elastomers with programmable supramolecular interactions and oriented crystalline microstructures. Nat Commun 10:1315/1–1315/8
22. Stockmann PN, Pastoetter DL, Woelbing M, Falcke C, Winnacker M, Strittmatter H, Sieber V (2019) New bio-polyamides from terpenes: α-pinene and (+)-3-carene as valuable resources for lactam production. Macromol Rapid Commun 40:1800903/1–1800903/7
23. Fu YQ, Liang K, Zhao JB, Zhang ZY, Zhang JY (2019) Synthesis and properties of bio-based nonisocyanate thermoplastic polyoxamide-ureas. Ind Eng Chem Res 58:21513–21520
24. Wang Z, Wei T, Xue X, He MM, Xue JJ, Song M, Wu SZ, Kang HL, Zhang LQ, Jia QX (2014) Synthesis of fully bio-based polyamides with tunable properties by employing itaconic acid. Polymer 55:4846–4856
25. Willke T, Vorlop KD (2004) Industrial bioconversion of renewable resources as an alternative to conventional chemistry. Appl Microbiol Biotechnol 66:131–142
26. Kumar S, Krishnan S, Samal SK, Mohanty S, Nayak SK (2017) Itaconic acid used as a versatile building block for the synthesis of renewable resource-based resins and polyesters for future prospective: a review. Polym Int 66:1349–1363
27. Lopez-Carrasquero F, de Ilarduya AM, Cárdenas M, Carrillo M, Arnal ML, Laredo E, Torres C, Méndez B, Müller AJ (2003)

New comb-like poly(n-alkyl itaconate)s with crystalizable side chains. Polymer 44:4969–4979
28. Rwei SP, Way TF, Chiang WY, Tseng JC (2017) Thermal analysis and melt spinnability of poly(acrylonitrile-co-methyl acrylate) and poly(acrylonitrile-co-dimethyl itaconate) copolymers. Text Res J 88:1479–1490
29. He MM, Wang Z, Wang RG, Zhang LQ, Jia QX (2016) Preparation of bio-based polyamide elastomer by using green plasticizers. Polymers 8:257/1–257/19
30. Ali MA, Tateyama S, Kaneko T (2014) Syntheses of rigid-rod but degradable biopolyamides from itaconic acid with aromatic diamines. Polym Degrad Stab 109:367–372
31. Ali MA, Tateyama S, Oka Y, Kaneko D, Okajima MK, Kaneko T (2013) Syntheses of high-performance biopolyamides derived from itaconic acid and their environmental corrosion. Macromolecules 46:3719–3725
32. Qian ZG, Xia XX, Lee SY (2009) Metabolic engineering of Escherichia coli for the production of putrescine. Biotechnol Bioeng 104:651–662
33. van Duuren JBJH, Brehmer B, Mars AE, Eggink G, dos Santos VAPM, Sanders JPM (2011) A limited LCA of bio-adipic acid: manufacturing the nylon-6,6 precursor adipic acid using the benzoic acid degradation pathway from different feedstocks. Biotechnol Bioeng 108:1298–1306
34. Kleiner EK (1970) Antioxidants for polymers. Ger Offen DE 1961532 A
35. Ramesh C (1999) New crystalline transitions in nylons 4,6, 6,10, and 6,12 using high temperature X-ray diffraction studies. Macromolecules 32:3721–3726
36. Obadia MM, Jourdain A, Cassagnau P, Montarnal D, Drockenmuller E (2017) Tuning the viscosity profle of ionic vitrimers incorporating 1,2,3-triazolium cross-links. Adv Funct Mater 27:1703258/1–1703258/10